Proceedings of 12th European Conference on Turbomachinery Fluid dynamics
Paper ID: ETC2017-238 & Thermodynamics ETC12, April 3-7, 2017; Stockholm, Sweden

FLUTTER ANALYSIS OF AN EMBEDDED BLADE ROW WITH A HARMONIC BALANCE SOLVER

H.-P. Kersken, C. Frey, G. Ashcroft

German Aerospace Center (DLR), Institute of Propulsion Technology, Cologne, Germany,
email:{hans-peter.kersken, christian.frey, graham.ashcroft}@dlr.de

H. Schönenborn

MTU Aero Engines AG, Munich, Germany, email:harald.schoenenborn@mtu.de

ABSTRACT

Commonly, in the flutter analysis of a turbomachine blade row the blade row studied for stability is treated as isolated from its neighbouring blade rows. This approach neglects the effects caused by the reflection of upstream and downstream propagating waves at the neighbouring blade rows. These reflected waves are the source of additional unsteady forces at the blade surface which may have significant effects on the aeroelastic stability of the blade row. To take this influence in the flutter analysis of a blade row into account a coupled unsteady simulation of all rows considered has to be performed. The usual approach to solve for the unsteady flow with a non-linear time-domain solver is expensive in terms of computational resources. Especially if in a multi-row configuration the blade counts of the blade rows considered do not allow restricting the simulation to a few passages in each row. To solve for the unsteady flow field, in this paper an alternative approach based on the nonlinear frequency domain Harmonic Balance method is presented. In the frequency-domain the unsteady flow field can be approximated with a small number of relevant frequencies and the circumferential and temporal periodicity of the problem reduces the computational domain to a single passage per blade row only. The efficiency of this approach for flutter analysis in a multi-row configuration is demonstrated by applying it to an embedded rotor blade row.

KEYWORDS

harmonic balance, flutter analysis, blade row interaction

NOMENCLATURE

a	speed of sound	$\mathbf{q}$	conservative flow variables
$\mathbf{R}$	non-linear residual	t	time
ω	angular frequency of a harmonic	$\mathscr{F}$	Fourier transform
τ	pseudo-time	m	circumferential wavenumber
$\hat{\mathbf{q}}_k$	temporal Fourier coefficient of $\mathbf{q}$	k	harmonic index
$\hat{\mathbf{q}}_{\omega,m}$	circumferential Fourier coefficient of $\hat{\mathbf{q}}_k$	i	imaginary unit $\sqrt{-1}$
Ω	rotational speed of a blade row	V	cell volume
$\begin{pmatrix} x \\ r \\ \theta \end{pmatrix}$	cylindrical coordinates	$\begin{pmatrix} U^x \\ U^r \\ U^\theta \end{pmatrix}$	contravariant velocities

INTRODUCTION

Aeroelastic analysis is an integral aspect of the design of compressor and turbine components. To investigate such complex phenomena efficient numerical methods capable of accurately capturing the underlying unsteady interaction between the blades and the aerodynamic flow field are required. As the physical phenomenon of flutter is periodic in nature the associated numerical simulations are typically formulated in the frequency domain. These phenomena have traditionally been simulated based on linearized governing equations starting from linearized two-dimensional Euler equations to finally linearized three-dimensional compressible Navier-Stokes equations. Whilst highly efficient, the linearized approach does not take nonlinear phenomena into account. The Harmonic Balance method (Hall et al., 2002; Ekici and Hall, 2006; Gopinath et al., 2007; Sicot et al., 2012) allows frequency-domain methods to be applied to nonlinear, time-periodic phenomena whilst taking the nonlinear coupling of unsteady perturbations and the mean flow into account. However, the main motivation to employ a Harmonic Balance solver instead of a time-linearized solver for flutter analysis is the well known instability of linear solvers when pseudo-time-stepping methods are employed to solve the linearized equation (He, 2008). Furthermore, in contrast to nonlinear unsteady simulations in the time-domain, the Harmonic Balance method takes full advantage of the spatial periodicity of the problem even in a multi-row configuration. For flutter analysis, assuming all blades in a row to be identical, only a single passage per row has to be simulated for each inter blade phase angle of interest. When carrying out the same analysis with a nonlinear unsteady solver in the time-domain, the same spatial periodicity is required in each row. That means that not only do the pitches of neighbouring sectors have to be identical but additionally the accumulated phase shift of the signals phase angle must amount to a multiple of 360°. For this reason the computational domain has to be duplicated and in most configurations of industrial interest a full wheel simulation is necessary if the interactions of more than two blade rows should be studied. The importance of taking waves generated by the scattering effect at neighbouring blade rows into account has been shown for example by Schönenborn and Ashcroft (2014) and Zhao et al. (2015). If one is interested in examining the cause effect relation of such phenomena, insight into the physical interaction mechanisms can be gained relatively easily by enabling or disabling specific perturbations in a Harmonic Balance solver. With a time-domain solver, similar observations are hardly possible.

The paper is organized as follows: First we give a concise overview of the Harmonic Balanced algorithm we implemented. Then we discuss the transformation a signal undergoes at blade row interfaces when the adjacent blade rows rotate relative to each other. Finally, we present results of a simulation where the developed method is applied to a 1 1/2 stage compressor rig and discuss the efficiency of the Harmonic Balance solver compared to an unsteady nonlinear solver in time-domain.

HARMONIC BALANCE ALGORITHM FOR MOVING GRIDS

The Harmonic Balance solver has been developed in the framework of TRACE (Becker et al., 2010). TRACE is a parallel Navier-Stokes flow solver for structured and unstructured grids that has been developed at DLR's Institute of Propulsion Technology to model turbomachinery flows. TRACE solves the finite-volume discretization of the compressible Reynolds-averaged Navier-Stokes (RANS) equations in the relative frame of reference using a multi-block approach. For the present work it is sufficient to note that following the discretization of the spatial operators in the Navier-Stokes equations the following system of ordinary differential

equations is obtained

$$\frac{d\mathbf{q}}{dt} + \mathbf{R}\left(\mathbf{q}(t)\right) = 0 \tag{1}$$

where $\mathbf{q}$ is the vector of conservative variables, $\mathbf{R}$ is the discretized RANS residual vector and t denotes the physical time. For completeness we summarize the Harmonic Balance algorithm as it is implemented in TRACE here. For a detailed description see (Frey et al., 2014).

Time-periodic solutions of Eqn. (1) can be described by a limited number of solution harmonics, i.e.,

$$\mathbf{q}(x,t) = \mathrm{Re}\left[\sum_{k=0}^{K} \hat{\mathbf{q}}_k(x) e^{ik\omega t}\right] \tag{2}$$

where $\hat{\mathbf{q}}_k$ are the complex valued solution harmonics and ω is the fundamental angular frequency. In such cases it is computationally attractive to formulate the unsteady problem, Eqn. (1), in the frequency-domain, i.e., to consider

$$\mathbf{i}k\omega\hat{\mathbf{q}}_k + \widehat{\mathbf{R}(\mathbf{q})}_k = 0 \tag{3}$$

for only a finite number of harmonics, $k = 0, \ldots, K$. For configurations in which non-linearity can be assumed to be negligible the coupling between the harmonics of $\mathbf{q}$, imposed by the nonlinear nature of $\mathbf{R}$, can be neglected and one obtains $K+1$ independent equations for the solution harmonics and the time-mean solution field. Here the equations for the harmonics are linear and only for the time-mean solution a nonlinear equation has to be solved. However, if one is interested in nonlinear effects an alternative approach is required to model $\widehat{\mathbf{R}(\mathbf{q})}_k$. We compute $\widehat{\mathbf{R}(\mathbf{q})}_k$ as $\mathscr{F}\mathbf{R}(\mathscr{F}^{-1}\hat{\mathbf{q}}))|_k$ and therefore solve

$$\mathbf{i}k\omega\hat{\mathbf{q}}_k + \mathscr{F}(\mathbf{R}(\mathscr{F}^{-1}\hat{\mathbf{q}}))|_k = 0, \tag{4}$$

where $\mathscr{F}$ denotes the Discrete Fourier Transform (DFT) and $\mathscr{F}^{-1}$ its inverse. Eqn. (4) is solved in the frequency-domain to obtain the complex valued harmonics of the conservative variables $\hat{\mathbf{q}}_k$. To compute the harmonics of the RANS residual vector $\mathbf{R}$ the solution field vector is first reconstructed at N sampling points within the period of the base frequency ω from the Fourier coefficients of the conservative variables $\hat{\mathbf{q}}_k$ using the inverse DFT. With the reconstructed solution vectors the RANS residual vectors $\mathbf{R}$ are then computed at the N sampling points to enable the DFT of $\mathbf{R}$ to be computed, i.e., the $\widehat{\mathbf{R}(\mathbf{q})}_k$. Since the RANS residual $\mathbf{R}$ is evaluated in the time-domain the standard flux and discretization schemes from the underlying nonlinear solver can be used.

As a hybrid time- and frequency-domain method this approach has the advantage, over methods formulated purely in the time- or frequency-domain, of being able to employ not only the possibly highly nonlinear time-domain flux functions (and their stabilizing numerical limiters) but also highly accurate nonreflecting boundary conditions formulated in the frequency-domain (Giles, 1990). Particularly in the context of aeroelasticity or aeroacoustics boundary conditions are of the utmost importance. The implementation in TRACE of these boundary conditions is described by (Kersken et al., 2014).

For flutter analysis the approach described above has to be modified to deal with time-dependent meshes as described by (Ashcroft et al., 2014). The governing equations are solved by an implicit pseudo-time approach. Discretizing the pseudo-time operator using the first-order

Euler backward method and then linearizing the harmonic balance residual $\mathbf{R}^{\mathrm{HB}}$ in pseudo-time the following system of equations is obtained

$$\left[\left(\frac{1}{\Delta\tau}+\mathbf{i}k\omega\right)+\left.\frac{\partial\mathbf{R}}{\partial\mathbf{q}}\right|_{\hat{\mathbf{q}}_0^{(n)}}\right]\Delta\widehat{(V\mathbf{q})}_k^{(n)}=-R_k^{\mathrm{HB}}\left(\hat{\mathbf{q}}^{(n)}\right), \tag{5}$$

where

$$R_k^{\mathrm{HB}}\left(\hat{\mathbf{q}}^{(n)}\right)=\left[\mathbf{i}k\omega\left.\widehat{(V\mathbf{q})}\right|_k+\mathscr{F}(\mathbf{R}(\mathscr{F}^{-1}\hat{\mathbf{q}}))|_k\right],\quad \Delta\widehat{(V\mathbf{q})}_k^{(n)}=\widehat{(V\mathbf{q})}_k^{(n+1)}-\widehat{(V\mathbf{q})}_k^{(n)}. \tag{6}$$

Here n is the pseudo-time iteration counter and V denotes the time-dependent cell volume. The coupling terms have been neglected in the left-hand side and therefore it depends directly only on the time-mean solution $\hat{\mathbf{q}}_0^{(n)}$. As such the residual Jacobian $\frac{\partial\mathbf{R}}{\partial\mathbf{q}}$ is identical to that employed in the steady flow solver. The linear system of equations, Eqn. (5), is solved using either the incomplete lower upper (ILU) or successive over-relaxation (SSOR) methods.

In this work the Harmonic Balance solver is used as a much more stable replacement of a pseudo-time time-linearized solver which in principle can be used for flutter analysis. Only its ability of computing the propagation of harmonics related to the flutter frequency is of interest here. With the multiple harmonic set feature of the Harmonic Balance implementation (Frey et al., 2014) blade row interactions based on blade and vane passing frequency can be simulated simultaneously. This is of special interest if the flutter frequency and blade or vane passing frequencies are close to each other or when the influences of wakes and potential fields upstream or downstream of the studied blade row have to be considered.

BLADE ROW COUPLING

In this section we summarize the approach used for transferring harmonics across blade row interfaces. More details can be found in (Frey et al., 2014) and (Frey et al., 2015).

The coupling of the harmonics between adjacent blade rows is based on the circumferential Fourier decomposition of the temporal harmonics at the interface situated at the axial position x

$$\hat{\mathbf{q}}_k(x,r,\theta)=\sum_{m\in\mathscr{M}}\hat{\mathbf{q}}_{\omega,m}(x,r)e^{\mathbf{i}m\theta}, \tag{7}$$

where $\mathscr{M}$ is the set of circumferential wavenumbers of circumferential modes which are resolved by a given minimum of cells per wavelength in circumferential direction.

Consider now the situation depicted in Fig. 1. In a neighboring blade row with relative rotational speed $\Omega'-\Omega$ a mode scattering occurs. Each circumferential mode $\hat{\mathbf{q}}_{\omega,m}(x,r)$ characterized by a circumferential wavenumber m, angular frequency ω and amplitude $\hat{\mathbf{q}}_{\omega,m}$ will be transformed to a mode with possibly different frequency, circumferential wavenumber and amplitude according to

$$\begin{aligned}\omega'=|\omega+m(\Omega'-\Omega)|,\quad m'&=\begin{cases}m, & \text{if } \omega+m(\Omega'-\Omega)\geq 0\\ -m, & \text{if } \omega+m(\Omega'-\Omega)<0\end{cases},\\ \widehat{\mathbf{q}'}_{\omega',m'}&=\begin{cases}\hat{\mathbf{q}}_{\omega,m}, & \text{if } \omega+m(\Omega'-\Omega)\geq 0\\ \overline{\hat{\mathbf{q}}_{\omega,m}}, & \text{if } \omega+m(\Omega'-\Omega)<0\end{cases}.\end{aligned} \tag{8}$$

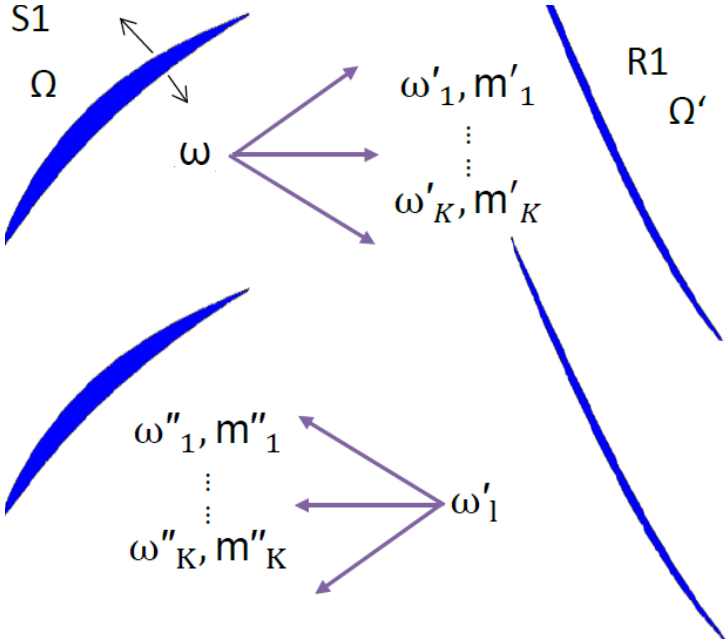

Figure 1: Mode scattering.

Here $\overline{\hat{\mathbf{q}}_{\omega,m}}$ is the complex conjugate of $\hat{\mathbf{q}}_{\omega,m}$. These transformations are applied to all harmonics including those of the mean solution. Equation (8) shows that the frequencies of the harmonics transformed into the adjacent blade row are in general not higher harmonics of the flutter frequency. This is the case only if the rotational speed of the rows coincide or more generally if $|m(\Omega' - \Omega)| = N\omega$ where N is an integer. These scattered modes may be reflected back into the row they originate from and thereby scattered again. All blade row interfaces as well as entries and exits are treated by 2D nonreflecting boundary conditions which are based on the dispersion relation of the linearized two-dimensional Euler equations, see (Kersken et al., 2014) for details. The boundary conditions allow for the prescription of incoming perturbations. In the case of a blade row interface, these perturbations are the circumferential modes that are the communicated modes given by Eqn. (7) from the adjacent blade row, taking into account the transformations of frequency, wave number and mode amplitudes described above. This is the key feature which allows to retain only one passage per blade row. The same spatial periodicity is not required because we are working in the frequency-domain here and passing amplitudes of circumferential decomposed temporal modes from one blade row to the other instead of flow states at a given instance in time. Note that those modes which do not have a counterpart in the opposite blade row, i.e., those which are not solved for there, are treated with the two-dimensional nonreflecting boundary conditions. In case of a 3D configuration the procedure described is applied on radial bands at the interfaces.

For modes passing through the interface and scattered back from the adjacent blade row we have due to the symmetry of Eqn. (8)

$$\omega''(\omega', m') = \omega, \quad m''(\omega', m') = m. \tag{9}$$

This shows that all scattered modes generated by the harmonic corresponding to the flutter mode contribute to this harmonic when reflected back into the blade row where the harmonic is generated. Based on the 2D theory cited above the propagation properties of modes with a specific

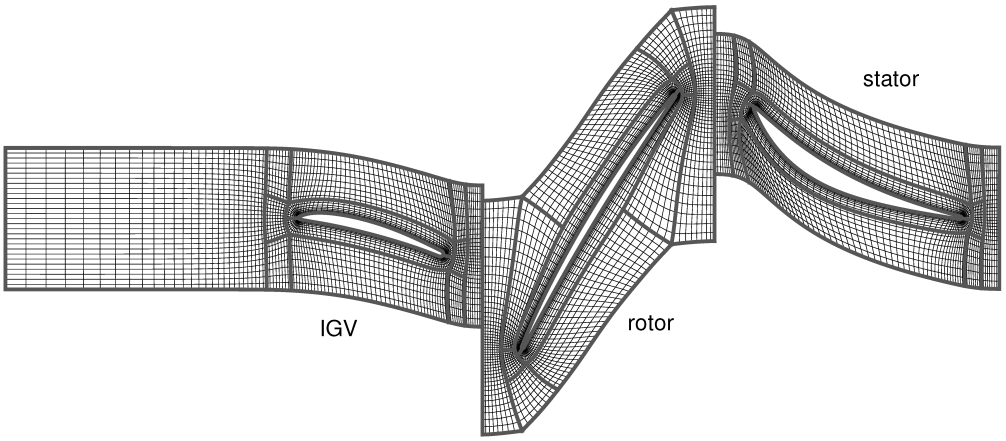

Figure 2: Mesh and block topology.

circumferential wavenumber and angular frequency can be derived at blade row interfaces. To identify cut-on modes which propagate into the neighbouring blade row we use the cut-off ratio given by

$$\zeta(m,\omega) = \left|\frac{\omega_c}{\tilde{\omega}}\right| = \left|\frac{\frac{m}{r}\sqrt{(a^2 - U_{mer}^2)}}{\omega + mU^\theta}\right| \tag{10}$$

where $U^\theta = U_\theta/r$ denotes the angular circumferential speed, $U_{mer} = \sqrt{U^{x2} + U^{r2}}$ is the meridional velocity, $\tilde{\omega}$ is the swirl modified angular frequency and ω_c is the cut-off frequency (Morfey (1971)). Note, if $U_\theta = -\Omega r$, $\tilde{\omega}$ is simply the disturbance frequency in the absolute from of reference. Modes are cut-off if $\zeta > 1$ while $\zeta < 1$ indicates that the mode is a cut-on mode that propagates into the neighbouring blade row unattenuated. The cut-on modes are generally considered to be the most important modes concerning back scattering effects. However, depending on the axial gap between the blade rows, the amplitude and the imaginary part of the axial wavenumber, which determines the speed of the decay, cut-off modes may be important as well. In this work we consider cut-on modes only.

APPLICATION

Configuration

The configuration chosen to demonstrate the efficiency of the method is a radial section close to the tip of a 1 1/2 stage compressor rig . The operation point is chosen such that cut-on acoustic waves originate in the rotor and propagate into the neighbouring blade rows. They are reflected there and influence the flutter behaviour of the rotor blade. Figure 2 shows the computational grid and the block topology for one passage per blade row containing. Every grid vertex is show for this radial cut and five cells are used in radial direction. The blade counts are 40 for the IGV upstream of the rotor and the stator downstream of the rotor and 24 for the rotor. The rotational speed of the rotor is 14968 rotations per minute. The structural mode is the first flexural mode with a frequency of 1752.9Hz. The flow in the rotor is transonic with an inlet mach number of about 0.78 in the rotating system. This relatively small configuration (a single passage of each row comprises about 15000 cells) is intended to serve as a demonstrator for simulating multi-row effects for flutter analysis by means of a Harmonic Balance solver. The Harmonic Balance method itself is not restricted to 2D cases as has been demonstrated for example in

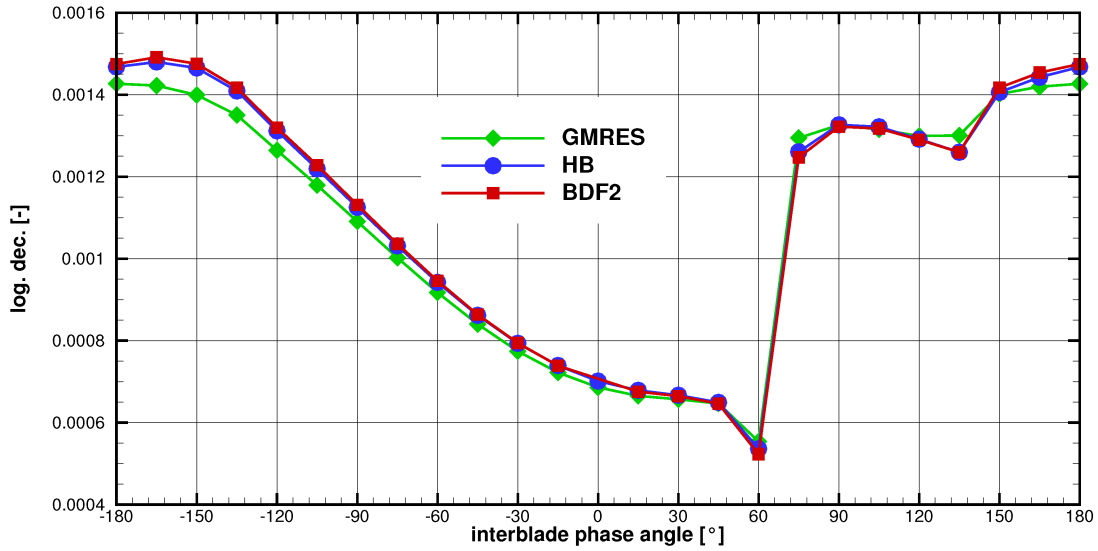

Figure 3: Aerodynamic damping (logarithmic decrement) for isolated rotor.

(Frey et al., 2015). A study where the proposed method is applied to a 3D configuration of industrial relevance is published in (Schönenborn, 2017).

Simulation Results

In this section we discuss the results obtained for the single blade row, rotor only, simulation taking into account one neighbouring blade row and both neighbours simultaneously. We compare the results of the Harmonic Balance solver with the nonlinear unsteady solver results and, in the single blade row case, with results obtained with the time-linearized solver. Finally, we will access the performance of the Harmonic Balance solver compared to the time-domain nonlinear solver.

Rotor only

The results in Fig. 3 show an excellent agreement of the Harmonic Balance and the nonlinear unsteady simulation employing a second order Euler backward time-stepping (marked as HB and BDF2, respectively). In the BDF2 simulation 64 time steps per period with 20 subiterations have been used. This indicates that the nonlinear effects present are correctly captured by the Harmonic Balance solver. However, this excellent agreement can be achieved only if consistent boundary conditions are used for the unsteady nonlinear solver and Harmonic Balance solver as described by Kersken et al. (2014) where the comparison has been carried out for a few inter blade phase angles only. As reference the figure displays results obtained with the time-linearized solver (labeled GMRES) as well. The small difference between the results obtained with the nonlinear and the time-linearized solvers shows that the linear approximation is valid for this case.

Rotor-Stator

As in the previous case a single passage in each blade row suffices for the simulation using the Harmonic Balance solver. The harmonics which have to be transferred into the neighbouring

blade row are determined using Eqn. (10) based on a steady simulation which gives the mean flow values at the interface. If the downstream situated stator S1 is taken into account the minimal damping at an inter blade phase angle of 60° is reduce by about 30%. To validate the results with the nonlinear solver a setup with the same sector size in both blade rows has been created and solved with a second order Euler backward time-stepping algorithm with 128 time steps per rotational period employing 20 subiterations per time step. For inter blade phase angles of $0°$and $\pm 120°$a mesh covering $1/8$ of the full wheel can be used comprising 3 rotor blades and 5 stator blades. For an inter blade phase angle of $\pm 60°$a quarter wheel and for $\pm 30°$and $\pm 90°$a half-wheel setup would be necessary while all other inter blade phase angles would require a full wheel simulation. We restrict the comparison therefore to the $0°$and $\pm 120°$cases. The computed damping values with the time-domain nonlinear solver for an inter blade phase angles of $\pm 120°$and $0°$are shown in Fig. 4. In contrast to the rotor-only setup where for the time-domain solver and the Harmonic Balance solver consistent boundary conditions could be employed here different implementations must be used. While for the Harmonic Balance solver the same implementation is applicable for the nonlinear time-domain solver a different implementation must be employed because the frequency-domain boundary conditions for the time-domain solver require to specify a unique frequency which in general is the blade or vane passing frequency. For flutter analysis, however, the flutter frequency comes into play as well. In this case only one of the frequencies can be handled appropriately. The other is not treated correctly which results in numerical reflections at the interfaces. The use of different boundary condition explains the larger differences between the Harmonic Balance results and the results obtained with the time-domain nonlinear solver compared to the single blade row simulation. Nevertheless, the overall agreement of the results is quite good.

Including the IGV

Adding the IGV to the configuration does not complicate the set-up for the Harmonic Balance solver much. Again only a single passage in all blade rows is necessary. This special case would allow one to use a time-domain nonlinear solver here as well because IGV and stator have the same blade count. If this would be not the case approximations like scaling the number of blades would be necessary. Adding the IGV to the configuration changes the characteristics of the damping curve significantly indicating that the upstream situated IGV has an overall larger influence on the flutter stability than the downstream situated stator. It displays a larger damping at the inter blade phase angle with the minimal damping but reduces the damping significantly close to the inter blade phase angle of $-60°$.

Computational Efficiency

For the rotor-stator case we compared the computational efficiency of the time-domain solver and the Harmonic Balance solver for the inter blade phase angles of $0°$and $\pm 120°$. All simulation have been carried out on 32 cores. In case of the time-domain simulation the computed damping has been taken from the $10th$ simulated rotation period. The computation time was about 30 minutes independent of the inter blade phase angle. In case of the Harmonic Balance solver the convergence depended on the inter blade phase angle and varied from about 14 minutes for the inter blade phase angles $0°$and $-120°$to 17 minutes for the $120°$case. Although fewer revolutions may suffice for the time-domain simulation to compute the average one should keep in mind that the case is the most favourable one for the time-domain solver concerning the number of passages used. All other inter blade phase angles require larger sec-

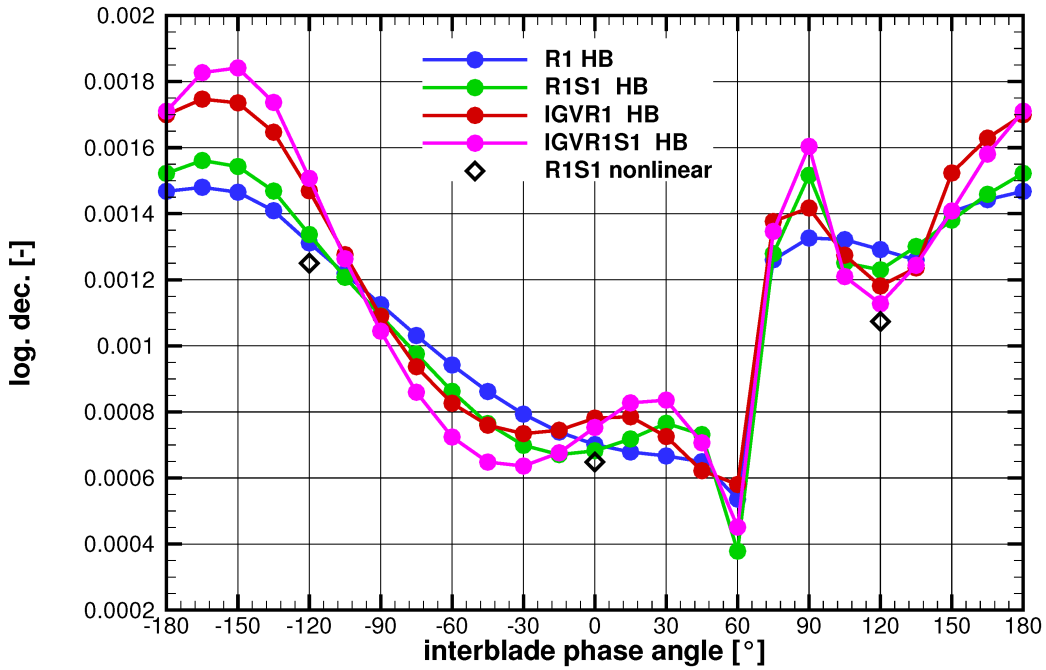

Figure 4: Aerodynamic damping (logarithmic decrement) for the embedded rotor.

tions of the full wheel with respective longer computation times. It can be estimated based on the cell count to be about 8 hours in case of a full wheel simulation which is necessary for all inter blade phase angles except those mentioned above to require a quarter or eight wheel only. Thereby the time for setting up different computational meshes has not been taken into account. For the Harmonic Balance solver the same, single passage, mesh can be used for all inter blade phase angles. Furthermore, no additional post processing is required to obtain the time averaged damping.

CONCLUSIONS

A Harmonic Balance algorithm for flutter analysis has been developed which can be applied to multi-row configurations. Effects on the damping caused by waves generated by the blade movement and reflected from adjacent blade rows can be easily accounted for. It has been shown that compared to a time-domain solver for multi-row configurations the setup is simplified and it is computationally more efficient. This is mostly due to the fact that the computational domain can be reduced to a single passage per blade row. Nonlinear effects caused by rotor-stator interactions with frequencies derived from blade and vane passing frequencies can be incorporated by applying the multiple harmonic set approach.

ACKNOWLEDGEMENTS

This research was supported by the German Federal Ministry of Economic Affairs and Energy under grant numbers 03ET7040C as part of the AG Turbo project COOREFLEX.

REFERENCES

Ashcroft, G., Frey, C., and Kersken, H.-P. (2014). On the development of a harmonic balance method for aeroelastic analysis. In *6th European Conference on Computational Fluid Dynamics (ECFD VI)*.

Becker, K., Heitkamp, K., and Kügeler, E. (2010). Recent progress in a hybrid-grid CFD solver for turbomachinery flows. In *Proceedings Fifth European Conference on Computational Fluid Dynamics ECCOMAS CFD 2010*.

Ekici, K. and Hall, K. C. (2006). Nonlinear frequency-domain analysis of unsteady flows in turbomachinery with multiple excitation frequencies. *Collection of Technical Papers - AIAA Applied Aerodynamics Conference*, 1:623–636.

Frey, C., Ashcroft, G., and Kersken, H.-P. (2015). Simulations of unsteady blade row interactions using linear and non-linear frequency domain methods. In *ASME Turbo Expo 2015: Turbine Technical Conference and Exposition*, volume 2B: Turbomachinery.

Frey, C., Ashcroft, G., Kersken, H.-P., and Voigt, C. (2014). A harmonic balance technique for multistage turbomachinery applications. In *Proceedings of ASME Turbo Expo 2014*.

Giles, M. B. (1990). Nonreflecting boundary conditions for Euler calculations. *AIAA Journal*, 28(12):2050–2058.

Gopinath, A., van der Weide, E., Alonso, J., Jameson, A., Ekici, K., and Hall, K. (2007). Three-dimensional unsteady multi-stage turbomachinery simulations using the harmonic balance technique. In *45th AIAA Aerospace Sciences Meeting and Exhibit, Reno, NV, January 8-11 2007*.

Hall, K. C., Thomas, J. P., and Clark, W. S. (2002). Computation of unsteady nonlinear flows in cascades using a harmonic balance technique. *AIAA Journal*, 40(5):879–886.

He, L. (2008). Harmonic solution of unsteady flow around blades with separation. *AIAA Journal*, 46(6):1299–1307.

Kersken, H.-P., Ashcroft, G., Frey, C., Wolfrum, N., and Korte, D. (2014). Nonreflecting boundary conditions for aeroelastic analysis in time and frequency domain 3D RANS solvers. In *Proceedings of ASME Turbo Expo 2014*.

Morfey, C. F. (1971). Sound transmission and generation in ducts with flow. *Journal of Sound and Vibration*, 14(1):37–55.

Schönenborn, H. (2017). Analysis of the effect of multi-row and multipassage aerodynamic interaction on the forced response variation in a compressor configuration - part 1: Aerodynamic excitation. In *Proceedings of ASME Turbo Expo 2017*. submitted.

Schönenborn, H. and Ashcroft, G. (2014). Comparison of non-linear and linearized cfd analysis of the stator-rotor interaction of a compressor stage. In *Proceedings of ASME Turbo Expo 2014*.

Sicot, F., Dufour, G., and Gourdain, N. (2012). A time-domain harmonic balance method for rotor/stator interactions. *Journal of Turbomachinery*, 134(1):011001.

Zhao, F., Nipkaut, J., and M.Vahdati (2015). Influence of acoustic reflection on flutter stability of an embedded blade. In *Proceedings of 11 th European Conference on Turbomachinery Fluid dynamics & Thermodynamics*.